

Two-neutron elastic transfer ${}^4\text{He}({}^6\text{He}, {}^4\text{He}){}^6\text{He}$ at $E = 151$ MeV

 I.V. Krouglov^{1,2,a}, M. Avrigeanu³, and W. von Oertzen^{1,4,b}
¹ Hahn-Meitner-Institut Berlin, Glienicke Strasse 100, 14109 Berlin, Germany

² St. Petersburg State University, Nuclear Physics Department, Uljanovskaja str. 1, 198904 St. Petersburg, Russia

³ “Horia Hulubei” National Institute for Physics and Nuclear Engineering, P.O. Box MG-6, 76900 Bucharest, Romania

⁴ Freie Universität Berlin, Fachbereich Physik, Arnimallee 14, 14195 Berlin, Germany

Received: 29 October 2001

Communicated by W.F. Henning

Abstract. Using the framework of the coupled reaction channels (CRC) the elastic scattering and the elastic transfer in the system ${}^6\text{He} + {}^4\text{He}$ measured at $E = 151$ MeV have been analysed. It is shown that the structure observed in the backward range of the angular distributions is influenced by the interference of the elastic 2n-transfer with a two-step process passing through the 2^+ excitation in ${}^6\text{He}$. The two-neutron transfer mechanism is studied in the microscopic approach and it is found that for the ground-state transition the one step dominates by a factor 10 over the two-step mechanism at this energy.

PACS. 24.10.Eq Coupled-channel and distorted-wave models – 25.70.Bc Elastic and quasielastic scattering – 25.60.Bx Elastic scattering

1 Introduction

The structure of ${}^6\text{He}$ has been studied with various reactions recently [1,2]. The unusual features of this nucleus are related to the fact that the odd isotope ${}^5\text{He}$ is unbound and that the ${}^6\text{He}_{0^+}$ bound ground state is formed by a three-body state also referred to as a “Borromean” nucleus. The two-neutron transfer has recently been measured [2–4], and the elastic 2n-transfer process in the system $\alpha + {}^6\text{He}$ has been reported by two different groups [5,6].

We present here the results on a coupled reaction channels analysis of the two-neutron transfer at high energy of $E_{\text{lab}} = 151$ MeV observed [2,5] in the reaction ${}^4\text{He}({}^6\text{He}, {}^4\text{He}){}^6\text{He}$. The backward rise in the angular distribution of the elastic channel evidenced in the experimental data is the signature of the well-known elastic-transfer process [7]. At this high incident energy the main processes are the break-up, the one-neutron transfer, the inelastic excitation of the 2^+ state (and of the continuum) and finally, the 2n-transfer, which appears as a backward rise in the elastic-scattering distribution. In the previous studies of this system, the predominance of the “di-neutron” transfer has been established [2] by using two types of wave functions. Corresponding experiments at high energy for the scattering of ${}^6\text{Li} + {}^4\text{He}$ [8] contain virtually

the same information as the data discussed here, namely a very strong backward rise due to the deuteron exchange.

The present analysis will concentrate on the elastic-transfer process and possible higher-order coupling aspects [9,10] and less on the details of the two-neutron wave functions.

With modern computer codes the coupled reaction channel (CRC) approach [11] can be used with a minimum of assumptions for the elastic two-neutron transfer as in the case of the ${}^4\text{He}({}^6\text{He}, {}^4\text{He}){}^6\text{He}$ reaction. In a recent study of the ${}^{12}\text{C}({}^6\text{He}, {}^4\text{He}){}^{14}\text{C}$ reaction at low energies, we obtained a very good description of the data using known parameters and known single (and two)-neutron spectroscopic factors [12]. Also the absolute values are very well reproduced considering the additional factor $(1.54)^2$ for the spectroscopic factors recently proposed for the two-neutrons in ${}^6\text{He}$ in refs. [13,14].

For the wave functions of ${}^5,6\text{He}$ and the structural aspects of the sequential transfer we will rely on these previous studies [12], in addition the di-neutron (“cluster”) approximation for the transitions via the inelastic channel will be considered. At high energy the excitation of the 2^+ state is expected to be very strong. This will give rise to the “indirect” contribution [9] in the 2n-transfer via this state and there will be a superposition of two amplitudes contributing to the ground state, as depicted in fig. 1.

The generalised double-folded potential for the real potential has been used, with the density-dependent BDM3Y-Paris effective nucleon-nucleon (NN) interaction

^a e-mail: krouglov@nuclpc1.phys.spbu.ru

^b e-mail: oertzen@hmi.de

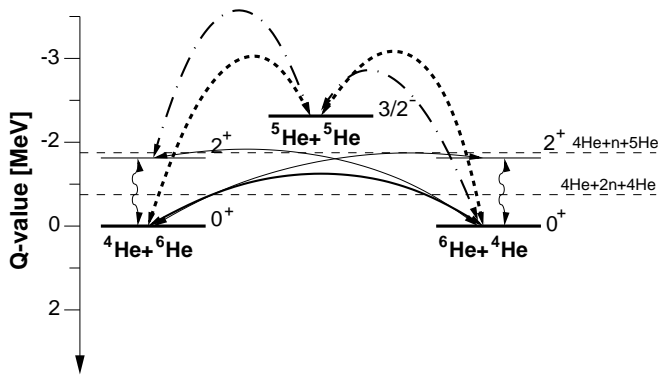


Fig. 1. Coupling diagram for one- and two-neutron transfer and inelastic excitation in the system ${}^6\text{He} + {}^4\text{He}$. The one- and two-step processes in the two-neutron transfer, the transitions via the ground state and the ${}^6\text{He}_{2+}$ state are indicated; the two-step route to the latter is not shown. The “indirect” routes via the inelastic excitation of the 2^+ state in the sequential mode are shown by dash-dotted line (the latter only in one direction). The thresholds indicate the binding of the 2n-cluster and of the neutron in the ${}^6\text{He}_{2+}$ state.

[15–17], and the imaginary part from Bachelier *et al.* [8] has been chosen in the optical potential in the incident and exit channels in the CRC calculations. Thus, we have good conditions to make a quantitative comparison of the CRC calculations with the experimental data.

2 CRC approach for the elastic transfer

The main aim of the present study is to test the dynamical properties of the ${}^6\text{He}$ -induced elastic and inelastic two-neutron transfer reactions. The elastic transfer has a Q -value equal to zero, which favours dynamically the transfer of the neutrons as a “cluster”. The sequential transfer of the two neutrons proceeds via the ${}^5\text{He} + {}^5\text{He}$ channel as an intermediate step. The negative Q -value for breaking the neutron pair and the weak binding of the neutron in the intermediate step makes the two-step process less probable [18–20] at this high energy. We will further include the reaction proceeding via the first excited 2^+ state of ${}^6\text{He}$ at 1.80 MeV which is 0.975 MeV above the 2-neutron threshold (but just a few keV below the ${}^5\text{He} + \text{neutron}$ break-up channel). These energies are depicted in fig. 1.

The coupling scheme is illustrated in fig. 1. The coupling routes discussed in the work calculations are the following: a) elastic two-neutron one-step (or cluster) transfer without inelastic excitation, solid line; b) cluster 2n-transfer with the “indirect” route via the 2^+ state, dash-dotted line, and thin line, the wavy line indicating inelastic excitation. The results of these calculation are shown in fig. 2. Then we have used c), the “microscopic” approach for the one and two-step neutron transfer (thick line, and thick dashed line). In order not to make the figure too complicated we have omitted the coupling routes via the 2^+ state in the backward direction from the exit channel, however, no direct coupling between the 2^+ states has been considered.

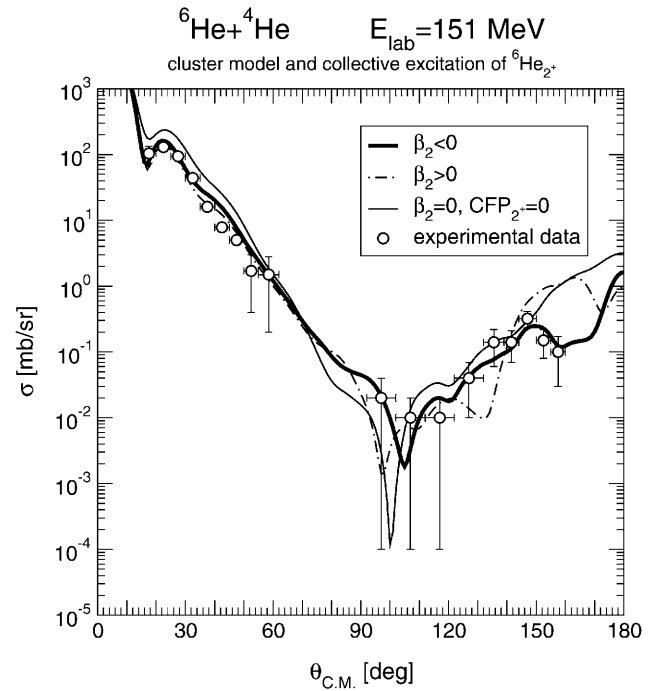


Fig. 2. Angular distributions of the elastic scattering of ${}^6\text{He} + {}^4\text{He}$ at $E_{\text{lab}} = 151$ MeV from ref. [2] and results of calculations. The curves show the following calculations: a) thin curve: elastic transfer with the 2n-cluster approximation as ref. [2], b) dot-dashed curve: elastic transfer with the indirect route and the “wrong” sign of the deformation parameter and c) thick curve: elastic scattering with elastic transfer including the indirect route via the 2^+ state of ${}^6\text{He}$ (see text).

The resonance for $n + {}^4\text{He}$ in ${}^5\text{He}(p_{3/2})$ is at an energy of 0.89 MeV with a width of 600 keV. However, in our calculation we use, as previously [12], the quasi-bound approximation for this state and the 2^+ state, because the differences to the exact treatment were rather small. For the microscopic description the one and two-neutron transfer channels are included, although the ${}^5\text{He} + {}^5\text{He}$ channel cannot be observed. The one-step and two-step two-neutron transfer routes via the ${}^6\text{He}_{2+}$ state are also drawn, as well as the 2n-cluster transfer route via the ${}^6\text{He}_{2+}$ state. The sequential transfer proceeds in both cases via ${}^5\text{He}$ channel, and we show it in fig. 1 with the relevant Q -values.

The *elastic transfer* of nucleons has been studied repeatedly in the last 25 years [7], a more recent example, with a rather complicated coupling scheme is the system ${}^{37}\text{Cl} + {}^{36}\text{S}$, where the full coupling effects of elastic and inelastic proton transfer have been studied [21]. The important aspect of the elastic transfer is the coherent addition of elastic potential scattering and the transfer amplitudes written as [7]

$$\sigma_{\text{elast}}(\theta) \propto [f_{\text{pot}}(\theta) + f_{2n}(\pi - \theta)]^2, \quad (1)$$

which gives rise to a characteristic interference pattern in the angular region, where the two amplitudes are of equal magnitude, due to the cross term which will appear

in eq. (1). But, according to [9], an additional amplitude can come into play with the second-order route via the ${}^6\text{He}_{2+}$ state, which will interfere with the normal transfer amplitude. The inelastic excitation has to be calculated, however, in higher order, we use the collective form factor with the di-neutron cluster transfer for this route. The complete microscopic approach will be given in later publication. If we use the microscopic description for the inelastic scattering and the transfer, there are big contributions in higher order from the back coupling into the entrance channel from the 1n-transfer channel. In this case many iterations are necessary in order to obtain convergence for the final result.

2.1 Wave functions

In the present work apart from the cluster approximation, the microscopic approach for the two-neutron transfer has been tested using the “standard” approach [12], where the transfer process is treated in the coupled reaction channel scheme [11] and the single-neutron and two-neutron transfer are treated in a consistent way.

The matrix elements for the one-nucleon transfer are defined in the usual way by the overlap of the single-particle wave functions in the first (initial) step $\langle \Phi_{4\text{He}} | \Phi_{5\text{He}} \rangle = \phi_{1n}^i$ for ${}^5\text{He}$ overlap with ${}^4\text{He}$, and the overlap $\langle \Phi_{5\text{He}} | \Phi_{6\text{He}} \rangle = \phi_{1n}^f$ for the final step. The overlap of $\langle \Phi_{4\text{He}} | \Phi_{6\text{He}} \rangle = \phi_{2n}$ consists of the product of the two mentioned single-particle structures, which are the same for the microscopic one-step 2n- and for the sequential 1n transfer. The spectroscopic amplitudes are well known and are given in table 1. Here the two-nucleon overlap is directly determined by the spectroscopic amplitudes (CFPs) for the $p_{3/2}$ strength of the individual steps taken from refs. [13,14]. This treatment of two-nucleon transfer (without the indirect route) produces three coherent components, the sequential single-nucleon transfer-amplitude, the one-step amplitude for two neutrons and the non-orthogonality term. The coherent sum gives the differential cross-section.

Table 1. Spectroscopic amplitudes for overlaps of one- and two-neutron wave functions for ${}^{5,6}\text{He}$ states.

Overlap	$(p_{3/2})$	$(p_{1/2})$	Reference
$\langle {}^4\text{He} {}^5\text{He} \rangle_{0+}$	1.1	0.00	this work
	0.85	-0.07	ref. [14]
$\langle {}^5\text{He} {}^6\text{He} \rangle_{0+}$	-1.4	0.00	this work
	-1.4	0.00	ref. [14]
$\langle {}^4\text{He} {}^6\text{He} \rangle_{0+}$	$(p_{3/2})^2$	$(p_{1/2})^2$	
	-1.6 to 1.8	0.00	this work
	1.6	0.00	ref. [14]
$\langle {}^4\text{He} {}^6\text{He} \rangle_{2+}$	$(p_{3/2})^2$	$(p_{1/2})^2$	
	1.6	0.0	

Table 2. Parameters (WS-shape) of the imaginary optical potentials for the calculations BDM shown in figs. 2 and 3, with the (DFM) double-folding BDM3Y real potential.

Potentials	W	r_w	a_w
${}^6\text{He} + {}^4\text{He}$	(MeV)	(fm)	(fm)
2n-cluster/and	8.0	1.21	0.95
2 + exit channel	45.0	0.7	0.40
DFM-microscopic ^(a)	8.0	1.21	0.95

^(a) One + two steps.

A particular feature is that the ground state of the ${}^5\text{He}$ nucleus is a $p_{3/2}$ resonance at 0.89 MeV in the ${}^4\text{He}$ system, with a width of 600 keV, thus no data can be made available for the 1n-transfer cross-section in these studies. For the ${}^6\text{He}_{0+}$ state the maximal spectroscopic factor has been used and only one configuration has been considered, $(p_{3/2})^2$, also for the ${}^6\text{He}_{2+}$ state.

There is still an ambiguity with the Q -value of the intermediate step: we use the correct Q -value of the ${}^5\text{He}$ channel, but a quasi-bound approximation has been used for the ${}^5\text{He}$ ground state with a binding energy of 0.01 MeV as well as for the ${}^6\text{He}_{2+}$ state. This approximation seems to be rather good in view of the dominance of the $\ell = 1$ centrifugal barrier of the $p_{3/2}$ configurations, which produces a tail of the wave function rather independent of these binding energies, however, we use the correct asymptotic Q -values in the dynamical CRC calculation. For the two-neutron wave function of the ground state the asymptotic binding energy of 0.98 MeV has been taken.

For the CCBA-coupling scheme the “collective” form factor for the 2^+ state allows an exact solution of the coupling equations in inelastic scattering and multi-step Born approximation for the transfer. The strength of the quadrupole coupling in this case has been taken from the literature [22].

In the analysis we have to choose the potential for the quasi-bound state in ${}^5\text{He}$ and the bound state in the ${}^5\text{He}$ - ${}^6\text{He}$ channel. The relevant values for the central potential with Woods-Saxon shape are given in the table 3 (as compared to ref. [12] we have omitted the spin-orbit potentials, because they produce only small effects not relevant for this study).

2.2 Microscopic real potentials

An important ingredient for the calculations is the optical potential for elastic scattering. We have used a microscopic approach for the real part of the optical potential describing the ${}^6\text{He} + \alpha$ scattering in the double folding model. We calculated the folding potential with the density- and energy-dependent BDM3Y1-Paris effective nucleon-nucleon (NN)-interaction [15–17] and with the RIKEN [23] density distributions for the helium isotopes given in the framework of the harmonic-oscillator basis. Since the details of the folding procedure are given

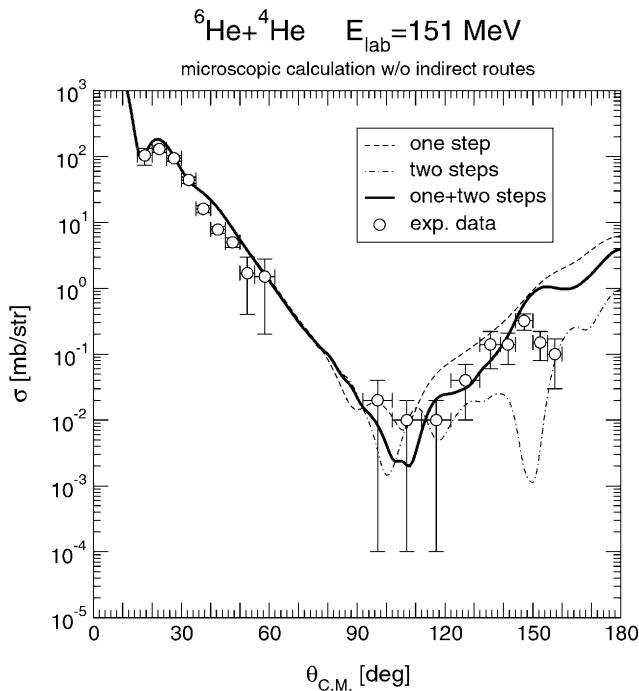


Fig. 3. Calculations of the elastic scattering with elastic transfer for ${}^6\text{He} + {}^4\text{He}$ as in fig. 2 at 151 MeV. The curves show the full calculations with two-step (sequential) and one-step transfer contributions for the two neutrons with parameters according to tables 1-2.

elsewhere [16], only the basic points are resumed in the following.

The energy- and density-dependent BDM3Y1 effective NN-interaction, as given in refs. [15–17], is used:

$$v^{\text{D(EX)}}(\rho, E, r) = g(E) F(\rho) v^{\text{D(EX)}}(r), \quad (2)$$

here the direct (D) and exchange (EX) components of the M3Y effective NN-interaction are based on the results of the G -matrix calculations using the Paris NN-potential $v^{\text{D(EX)}}(r)$, which is parametrised in terms of Yukawa functions. The energy-dependent factor is $g(E) = 1 - 0.003E$, and the density-dependent function $F(\rho)$ for the BDM3Y1 effective interaction is given by $F(\rho) = C(1 - \alpha\rho)$, considered as the best choice for the real folded potentials involving α -particles and other light ions [15,17].

For the calculation of the knock-on exchange term of the folded potential the approximation of Campi and Bouyssy [24] has been used. Therefore we preserved the first term of the expansion given by Negele-Vautherin [25] for the realistic density-matrix expression but replaced the Fermi momentum by the average relative momenta [24] as a function of the density distribution $\rho(r)$ and of the kinetic-energy density $\tau(r)$ for each participant in the interaction. Specifically for light nuclei the modified Thomas-Fermi approximation of Krivine-Treiner [26] has been considered for the kinetic-energy density [27].

Furthermore, the frozen-density approximation (which corresponds to the local density approach [16,17] in Hartree-Fock calculations) is used for the overlap den-

Table 3. Binding potentials for He-neutron bound states.

	V (MeV)	r (fm)	a (fm)
${}^5\text{He} + n$	-49.0	1.25	0.82
${}^4\text{He} + n$	-53.9	1.25	0.82
${}^4\text{He} + 2n$	-58.5	1.20	0.90
${}^4\text{He} + 2n(2^+)$	-71.5	1.20	0.90

sity, which enters with its explicit form into the density-dependent factor $F(\rho)$ (*i.e.* ρ being taken as the sum of the densities of the two colliding nuclei at the midpoint of the intra-nuclear separation).

In the data analysis we adopted the imaginary component of a phenomenological optical potential for ${}^4\text{He} + {}^6\text{Li}$ scattering from Bachelier *et al.* [8]. In the process of the analysis, we have found (as well as the authors of ref. [2]) that the imaginary part is relatively weak for this high energy. Variations of the imaginary part have shown that for stronger absorption strong diffraction structures are observed in the forward and backward part of the angular distribution, in contradiction with the data. We mention that the same (almost identical!) angular distributions are observed in the case of ${}^4\text{He} + {}^6\text{Li}$ scattering and the analysis of ref. [28] indicates also that the potential has become rather transparent at these energies. In both cases the data for the 2n- or (np)-transfer show a pronounced dip in the out-most angles. Also from our experience the description of these structures is not obtained with any reasonable change in the imaginary potentials, and thus in both cases [2,28] the authors fail to reproduce properly the 2n-transfer part of the angular distributions. We will show that this structure is naturally reproduced if the indirect route, the excitation of the 2^+ state is included. The final result needs a deformation parameter for the ${}^6\text{He}(2^+)$ state with a negative sign, and the fit can be fine tuned with the imaginary potential for the exit channel, the imaginary potential has to be changed to describe the larger absorption in the transfer process (the values are given in table 2).

3 Results of the calculation

3.1 Two-neutron transfer via inelastic excitation of the ${}^6\text{He}^{2^+}$ state

The inelastic scattering to the (2^+) state in ${}^6\text{He}$ at 1.80 MeV is expected to be quite strong. In addition some authors [29] are concerned with the excitation of unbound states (and of the continuum) in ${}^6\text{He}$. Both excitations can be phenomenologically incorporated by an adequate choice of the imaginary potential. The majority of the calculations in the cited refs. [2,6] have been done in this way. The ${}^6\text{He}_{2^+}$ state has been included in our calculation by introducing the collective form factor and a transition strength for the Coulomb interaction of $B(E2) = 3.2 \text{ e}^2\text{fm}^4$, as cited by Aumann *et al.* [22]. This

value has been used to calculate the deformation length δ_2 . Because of the very different radial shapes of the Coulomb, real and imaginary parts of the potentials, their corresponding deformation lengths $\delta_2 = \beta_2 R$ do vary in the range of 0.8 to 1.8 fm. The center-of-mass motion of the di-neutron is described by a wave function with $2N + L = 2$, so we have $N = 1$ and $L = 0$ for the ground state and $N = 0$ and $L = 2$ for the excited 2^+ state.

In the calculations we needed some fine tuning of the imaginary potential the parameters of which are given in table 2. The result of the calculations is shown in fig. 2. We note that similar to the calculations of ref. [2] the direct 2n-transfer (curve with $\beta_2 = 0$ without coupling to the 2^+ state) gives the correct absolute value of the cross-section, the calculation fails, however, to reproduce the maximum at $\theta_{c.m.} = 140^\circ$. The same failure is observed in the analysis of the ${}^6\text{Li} + {}^4\text{He}$ scattering at the same energy in ref. [28]. The inclusion of the indirect route with a deformation parameter β_2 gives a clear signal for the origin of this structure. In fact the interference of the direct and indirect routes produces a pronounced structure, the negative sign of β_2 gives the correct description. These interference phenomena are discussed for the 2n-transfer to the excited states in ref. [9].

The present description of the interference of the elastic transfer with its indirect route via the 2^+ state of ${}^6\text{He}$ would also be obtained for the elastic transfer in the ${}^6\text{Li} + {}^4\text{He}$ case [8, 28] with the inclusion of the excitation from the ground state 1^+ to the 3^+ state at 2.183 MeV in ${}^6\text{Li}$, which is the spin-isospin analog state of the 2^+ state of ${}^6\text{He}$, for this a $E2$ excitation with a $B(E2)$ -value of $21.8 \text{ e}^2\text{fm}^4$ is cited in ref. [30] (this gives a deformation length of approximately 2.7 fm). The observed structure in the backward rise in these data [8], was thus not reproduced in the calculations without the indirect route of ref. [28].

A final comment on the parameters of the calculation: the important ingredient in the interference phenomenon is the amplitude (and its sign) for the 2^+ excitation in ${}^6\text{He}$, which is actually an unbound state. We have treated it for the transfer as a bound state in the 2n-cluster approximation, however, we have chosen a strong imaginary part for the 2^+ channel (see table 2) in order to have a strong absorption to this channel. In the collective excitation of the 2^+ state, complex coupling has been applied, where this part of the potential also counts.

3.2 One- and two-step neutron transfer

As mentioned before the microscopic approach for the transfer of two neutrons contains three terms, the one-step, the sequential transfer and the non-orthogonality term. In addition in the present case the 2^+ state in ${}^6\text{He}$ in the microscopic basis gives rise to higher-order transitions, but with an inelastic transition preceding the mentioned processes. This fully microscopic approach will be discussed elsewhere.

We present here calculations for the 2n-transfer without the “indirect” route in the microscopic basis with the

parameters of the wave functions as given in tables 1 and 3, in order to illustrate the relative importance of the previously mentioned two contributions. In fig. 3 we show the result of the CRC calculations for the individual contributions and for their sum for the population of the (0^+) ground state in ${}^6\text{He}$. We notice a dominance of the one-step 2-neutron transfer contribution by one order of magnitude, and there is a destructive interference between the one- and two-step amplitudes. This observation is in accordance with the expectation that the 1n-transfer reactions between weakly bound states decreases with incident energy, because of the poor momentum overlap as discussed in refs. [18, 19]. This decrease of the cross-section becomes even more conspicuous for two-step processes, namely for 2n-transfer and charge exchange reactions like $({}^{12}\text{C}, {}^{12}\text{N})$, as discussed in ref. [20]. In contrast, the results of the present calculations for the 2-neutron transfer to the excited 2^+ state have shown, that there the sequential transfer dominates by a factor 100 and more, and that the one-step amplitude introduces also a destructive interference of the two amplitudes.

In general we notice that the sequential process may be still of importance, implying that the “di-neutron” structure is an effective description.

We have also made calculations with the inclusion for the “indirect routes” and the microscopic treatment of the 2n-transfer. These results will be discussed together with an analysis [31] of the low-energy data of ref. [6], where a very pronounced interference of the elastic scattering and the 2n-transfer is observed over the whole angular range.

4 Discussion and conclusions

In this work we have shown that the 2n-transfer plays a dominant role in the elastic scattering of ${}^6\text{He}$ on ${}^4\text{He}$. Using the microscopic approach we have obtained a satisfactory description of the absolute value of the two-neutron elastic transfer. The various spectroscopic amplitudes used in the present analysis are known from previous studies. For the real part of the optical potential we have chosen a parameter-free double-folding potential without renormalisation. Calculations for the elastic 2n-transfer between the ground states using the 2n-cluster approach or the microscopic description of the two neutrons are found to reproduce well the absolute values of cross-sections observed as the backward rise in the angular distributions of the elastic scattering. These calculations fail, however, to reproduce the pronounced structure observed in the data at the largest angles (the same problem occurred in the analysis of the ${}^4\text{He}$ on ${}^6\text{Li}$ scattering of refs. [8, 28]). The discrepancy is removed by introducing the 2n-transfer via the inelastic excitation of the (2^+) state of ${}^6\text{He}$ (indirect route). The interference of the direct 2n-transfer with the indirect route causes the mentioned additional interference structure, and reproduces the correct position of the minimum only with a deformation parameter of the (2^+) state with a negative sign. Such interference phenomena are actually well known from the two-nucleon

transfers to excited states studied some time ago, an account of these previous studies can be found in reviews of R. Ascuitto and E. Seglie [9] or of Tamura *et al.* [32]. A fully microscopic analysis of the ${}^6\text{He} + {}^4\text{He}$ scattering in the CRC framework including the data at low energy is preparation [31].

Two of the authors (I.V.K. and M.A.) are grateful to the Hahn-Meitner-Institut for the warm hospitality. This work has been supported in part by the European Commission Contract No. ICA1-CT-2000-70023/12.02.2001. We thank Dr. H.G. Bohlen for useful discussions.

References

1. M.V. Zhukov, B.V. Danilin, D.V. Fedorov *et al.*, *Phys. Rep.* **231**, 151 (1993).
2. Yu.Ts. Oganessian, V.I. Zagrebaev, J.S. Vaagen, *Phys. Rev. Lett.* **82**, 4996 (1999); *Phys. Rev. C* **60**, 044605 (2000).
3. A.N. Ostrowski, A.C. Shotton, W. Bradfield-Smith *et al.*, *J. Phys. G* **24**, 1553 (1998).
4. R. Wolski, A.S. Fomichev, A.M. Rodin *et al.*, *Phys. Lett. B* **467**, 8 (1999).
5. G.M. Ter-Akopian *et al.*, *Phys. Lett. B* **426**, 252 (1998).
6. R. Raabe, A. Piechaczek, A. Andreev *et al.*, *Phys. Lett. B* **458**, 1 (1999).
7. W. von Oertzen, H.G. Bohlen, *Phys. Rep.* **19**, 2 (1975).
8. D. Bachelier, M. Bernas, J.L. Boyard, H.L. Harney, J.C. Jourdain, P. Radvanyi, M. Roy-Stephan, R. Devries, *Nucl. Phys. A* **195**, 361 (1972).
9. R.J. Ascuitto, E. Seglie, in *Treatise on Heavy Ion Science*, edited by D.A. Bromley, Vol. **1** (Plenum Press, New York 1984) p. 463.
10. B.F. Bayman, J. Chen, *Phys. Rev. C* **26**, 1509 (1982).
11. Ian J. Thompson, *Comput. Phys. Rep.* **7**, 167 (1988).
12. I.V. Krouglov, W. von Oertzen, *Eur. Phys. J. A* **6**, 501 (2000).
13. N.K. Timofeyuk, I.J. Thompson, *Phys. Rev. C* **61**, 044608 (2001).
14. N.K. Timofeyuk, *Phys. Rev. C* **63**, 054609 (2001).
15. Dao T. Khoa, W. von Oertzen, *Phys. Lett. B* **304**, 8 (1993); **342**, 6 (1995).
16. D.T. Khoa, W. von Oertzen, H.G. Bohlen, *Phys. Rev. C* **49**, 1652 (1994).
17. Dao T. Khoa, G.R. Satchler, W. von Oertzen, *Phys. Rev. C* **56**, 954 (1997).
18. W. von Oertzen *et al.*, *Phys. Lett. B* **151**, 195 (1985).
19. H. G. Bohlen *et al.*, *Nucl. Phys. A* **488**, 89c (1988).
20. H. Lenske, H. Wolter, H.G. Bohlen, *Phys. Rev. Lett.* **62**, 1457 (1989).
21. W. von Oertzen, Th. Wilpert, B. Gebauer *et al.*, *Z. Phys. A* **358**, 395 (1997).
22. T. Aumann *et al.*, *Phys. Rev. C* **59**, 1252 (1999).
23. I. Tanihata, D. Hirata, T. Kobayashi, S. Shimoura, K. Sugimoto, H. Toki, Preprint RIKEN-AF-NP-123, April 1992; *Phys. Lett. B* **289**, 261 (1992).
24. X. Campi, A. Bouyssy, *Phys. Lett. B* **73**, 263 (1978).
25. J.W. Negele, D. Vautherin, *Phys. Rev. C* **5**, 1472 (1972).
26. H. Krivine, J. Treiner, *Phys. Lett. B* **88**, 212 (1979).
27. M. Avrigeanu, G.S. Anagnostatos, A.N. Antonov, J. Giapitzakis, *Phys. Rev. C* **62**, 017001 (2000); M. Avrigeanu, A.N. Antonov, H. Lenske, I. Şteţcu, *Nucl. Phys. A* **693**, 616 (2001).
28. T. Sinha, Subinit Roy, C. Samanta, *Phys. Rev. C* **48**, 785 (1993).
29. K. Rusek, K. W.Kemper *Phys. Rev. C* **61**, 034608 (2000).
30. F. Ajzenberg-Selove *Nucl. Phys. A* **490**, 1 (1988).
31. W. von Oertzen, I.V. Krouglov, in preparation.
32. T. Tamura, T. Ugagawa, M. Mermaz *Phys. Rep. C* **65** 345 (1980).